Electronic Supplementary Material (ESI) for ChemComm.

Supplementary Information

In-situ formed Co from Co-Mg-O solid solution synergizing with LiH for efficient ammonia synthesis

Wenbo Gao,[a] Sheng Feng,[a,b,c] Hanxue Yan,[a,b] Qianru Wang,[a,b] Hua Xie,[a] Ling Jiang,[a] Weijin Zhang,[a] Yeqin Guan,[a,b] Han Wu,[a,b] Hujun Cao,[a,b] Jianping Guo,[*a,b] and Ping Chen[a,b]

[a] Dalian National Laboratory for Clean Energy, State Key Laboratory of Catalysis, Dalian Institute of Chemical Physics, Chinese Academy of Sciences, Dalian 116023, China.

[b] University of Chinese Academy of Sciences, Beijing 100049, China.

[c] Zhang Dayu School of Chemistry, Dalian University of Technology, Dalian 116024, China.

Email: guojianping@dicp.ac.cn

Experimental Section

1. Chemicals.

Li metal (Alfa Aesar, 99.9%), Co powder (ca. 20 nm, Aladdin, 99.9%), $CoCl_2$ (Aldrich, 97%), $H_2C_2O_4 \cdot 2H_2O$ (Kermel, 99%), $Co(NO_3)_2 \bullet 6H_2O$ (Kermel, 99%), $Co(CH_3COO)_2 \bullet 2H_2O$ (Kermel, 99%), $Mg(CH_3COO)_2 \bullet 2H_2O$ (Kermel, 99%), N_2 (Dalian Special gases Co., 99.999%), H_2 (Dalian Special gases Co., 99.999%), Ar (Dalian Special gases Co., 99.999%) and liquid NH_3 (Dalian Special gases Co., 99.99%) were used as supplied. As Li metal and the prepared samples containing LiH are very sensitive to moisture and oxygen, sample preparation and loading were conducted in a glove box filled with Argon.

2. Preparation of catalysts.

The Co-Mg-O solid solution was prepared using the co-precipitation (Co-Mg-O-co) procedure. Firstly, oxalic acid ($H_2C_2O_4 \cdot 2H_2O$, 0.12 mol), cobalt acetate ($Co(CH_3COO)_2 \cdot 2H_2O$, *a* mol, $0 < a < 0.08$), and magnesium acetate ($Mg(CH_3COO)_2 \cdot 2H_2O$, (0.08-*a*) mol) were dissolved in 300 mL, 50 mL, and 100 mL deionized water, respectively. Secondly, the $Co(CH_3COO)_2 \cdot 2H_2O$ and $Mg(CH_3COO)_2 \cdot 2H_2O$ solutions were added drop by drop into the $H_2C_2O_4 \cdot 2H_2O$ solution. After aging for 10 h at 30 ℃, the resulting solid was filtrated and dried for 10 h at 100 ℃ before reducing at 470 ℃ for 5 h under a H_2 flow to obtain the Co-Mg-O-co solid solution sample. Following this procedure, the obtained solid solution was denoted as Co-*m*Mg-O-co (*m* is the molar ratio of Mg to Co). MgO was prepared as the same procedure as Co-Mg-O-co without the use of cobalt acetate. Co-Mg-O samples were also prepared by the methods of impregnation (denoted as Co-Mg-O-i) and deposition–precipitation (denoted as Co-Mg-O-p). The Co-Mg-O-i sample was obtained by impregnating homemade MgO with ethanol solutions of $Co(NO_3)_2 \cdot 6H_2O$ (Kermel, 99.0%), and then drying the mixture at 100 °C for 10 h after the ethanol evaporated completely at room temperature. Finally, the residue was reduced by H_2 at 470 °C for 5 h. The Co-Mg-O-p sample was obtained by precipitating $Co(NO_3)_2 \cdot 6H_2O$ on homemade MgO using urea as the precipitant. In a typical procedure,

$Co(NO_3)_2 \cdot 6H_2O$, homemade MgO, and urea were respectively added in 50 mL deionized water in a 100 mL flask. And then the solution was heated at 80 °C for 8 h. Subsequently, the solid product was separated by extraction filtration and then dried at 100 °C for 10 h. At last, the residue was reduced by H_2 at 470 °C for 5 h.

LiH/Co-Mg-O-co, LiH/Co-Mg-O-i, and LiH/Co-Mg-O-p catalysts were obtained via impregnating the corresponding Co-Mg-O supports in a lithium-ammonia solution (Li metal dissolved in liquid ammonia and converted to lithium amide), removing NH_3 by evacuating and then hydrogenating the solid at 300 °C and 10 bar of H_2 flow ($LiNH_2$ converted to LiH via the reaction $LiNH_2 + H_2 \rightarrow LiH + NH_3$).[1] Following this procedure, the as-prepared catalysts were denoted as *n*LiH/Co-*m*Mg-O (*m* and *n* are the molar ratio of Mg to Co and Li to Co, respectively). Typically, the molar ratio of Mg to Co and Li to Co are 3:1 and 5:1, unless otherwise emphasized. The Co-LiH composite catalyst was prepared by the ball milling method as previously reported.[2] The LiH/Co-co was prepared in the similar procedure to the LiH/Co-Mg-O-co catalyst without the addition of Mg acetate during the preparation process. LiH/Co and LiH/MgO were prepared as the same procedure as LiH/Co-Mg-O-co catalyst. The processes of impregnating LiH and ball milling should be isolated with oxygen and moisture.

3. Catalytic test.

NH_3 synthesis activity was tested on a quartz-lined stainless-steel fixed-bed reactor. Typically, 30 mg of catalyst was loaded into the reactor operating in the glovebox, and the temperature was raised at a ramping rate of 5 °C min^{-1} under the given pressure with a flow rate of 30 mL min^{-1} (N_2:H_2 = 1:3). Because the hydride is sensitive to oxygen and moisture, a reaction gas of high purity (99.999%) is used and is further purified by passing through a column filled with a Na-NaCl solid mixture. The NH_3 synthesis rate was measured with a conductivity meter (Mettler Toledo SevenMulti) by conducting the exhaust gas to a diluted sulfuric acid solution and calculating the change in conductivity with time. The activity data reported here were collected after at least 5 hours at the corresponding temperature. The NH_3 yield is calculated according to eqn. 1.

NH_3 yield (%) = 100*NH_3 produced (mol min^{-1}) / 2*N_2 supplied (mol min^{-1}) *(1)*

4. Kinetic measurements.

The N_2, H_2, NH_3 reaction orders were measured at 250 ℃ and 10 bar. The NH_3 reaction order (α) was obtained by changing the flow rate of syngas while keeping the molar ratio of N_2 to H_2 at 1:3. *r* is ammonia synthesis rate, *F* is total flow rate, *C* is a constant. The N_2 (β) and H_2 (γ) reaction orders were calculated by using two different methods. For the first one, the reaction orders were calculated according to the equations (5) and (6). In this case, the effect of variation of P_{NH3} was considered.

$$r = k P_{NH3}^{\alpha} P_{N2}^{\beta} P_{H2}^{\gamma} \quad (2)$$

$$lnP_{NH3} = 1/(1-\alpha)\ ln1/F + C_1 \quad (3)$$

$$lnr = lnk + \alpha\ lnP_{NH3} + \beta\ lnP_{N2} + \gamma\ lnP_{H2} \quad (4)$$

$$lnr - \alpha\ lnP_{NH3} = \beta\ lnP_{N2} + C_2 \quad (5)$$

$$lnr - \alpha\ lnP_{NH3} = \gamma\ lnP_{H2} + C_3 \quad (6)$$

For the other one, the reaction orders of N_2 and H_2 were obtained by using the equations (7) and (8) without considering the influence of the change of P_{NH3}. It is worth mentioning that the reaction orders of N_2 and H_2 in many literatures were obtained in this way. For convenient comparison, the reaction orders with or without considering the influence of change of P_{NH3} were both calculated and listed in **Table S2**.

$$lnr = \beta\ lnP_{N2} + C_4 \quad (7)$$

$$lnr = \gamma\ lnP_{H2} + C_5 \quad (8)$$

5. Characterization.

Powder X-ray diffraction (PXRD) patterns were recorded on a PANalytical X'pert diffractometer using a homemade sample cell covered with KAPTON film to avoid air and moisture contamination. Fourier-transform infrared (FTIR) spectra were recorded on a TENSOR II infrared spectrometer in diffuse reflectance FTIR (DRIFT) mode. The resolution is 4 cm^{-1}. TEM images were obtained on a Tecnai G2 F30 S-Twin transmission electron microscope (FEI Company). The sample was dispersed in

tetrahydrofuran (THF) and dropped on a carbon-coated copper TEM grid. XPS data were recorded using an ESCALAB 250xi electron spectrometer (ThermoFisher) with hν=1486.6 eV Al Kα radiation. The binding energies in the XPS analysis were internally standardized with respect to C 1s (284.8 eV). X-ray absorption spectra (XAS) for Co K-edge were recorded at the BL14W beamline of the Shanghai Synchrotron Radiation Facility (SSRF, 3.5 GeV electron energy, and 300 mA ring currents). The samples were pressed into pellets and then sealed with KAPTON film on both sides to avoid air or moisture contamination. The BET specific surface areas of catalysts were measured by N_2 physisorption at −196 °C on a Micromeritics ASAP2010 instrument. An inductively coupled plasma atomic emission spectrometer (ICP-AES, PerkinElmer ICP-AES 7300DV) was used to determine the content of Co and Li in the catalyst. Temperature-programmed reaction (TPR) measurements were performed in a quartz-lined stainless steel reactor, and the effluent gases were analyzed by an online mass spectrometer (Hiden HPR20). Gas-phase cluster measurement coupled with Mass Spectrometry was carried out using a homemade instrument with a laser vaporization source and a dual-channel time-of-flight mass spectrometer (D-TOFMS). Details of the experiment can be found in our previous studies.[4] Briefly, the gas-phase cluster species were generated via pulsed laser vaporization of the Co-LiH catalyst in the presence of a supersonic beam of carrier gas. Under the efficient cooling by the supersonic expansion of pulsed carrier gas, the clusters were cooled to ~200 K in the vacuum chamber and analyzed by the TOF mass spectrometer.

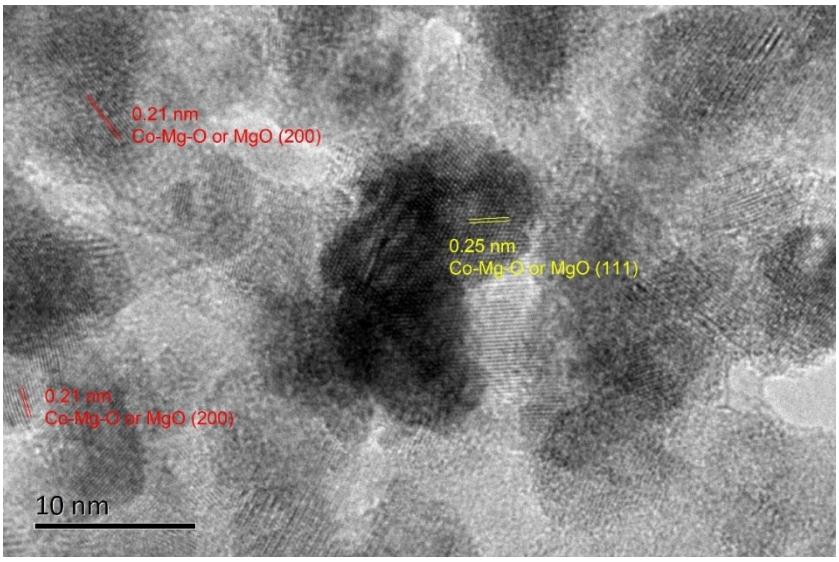

Figure S1. TEM image of the Co-Mg-O-co solid solution. The lattice fringes with distances of 0.25 and 0.21 nm are in agreement with the (111) and (200) lattice spacing of MgO or Co-Mg-O-co solid solution.

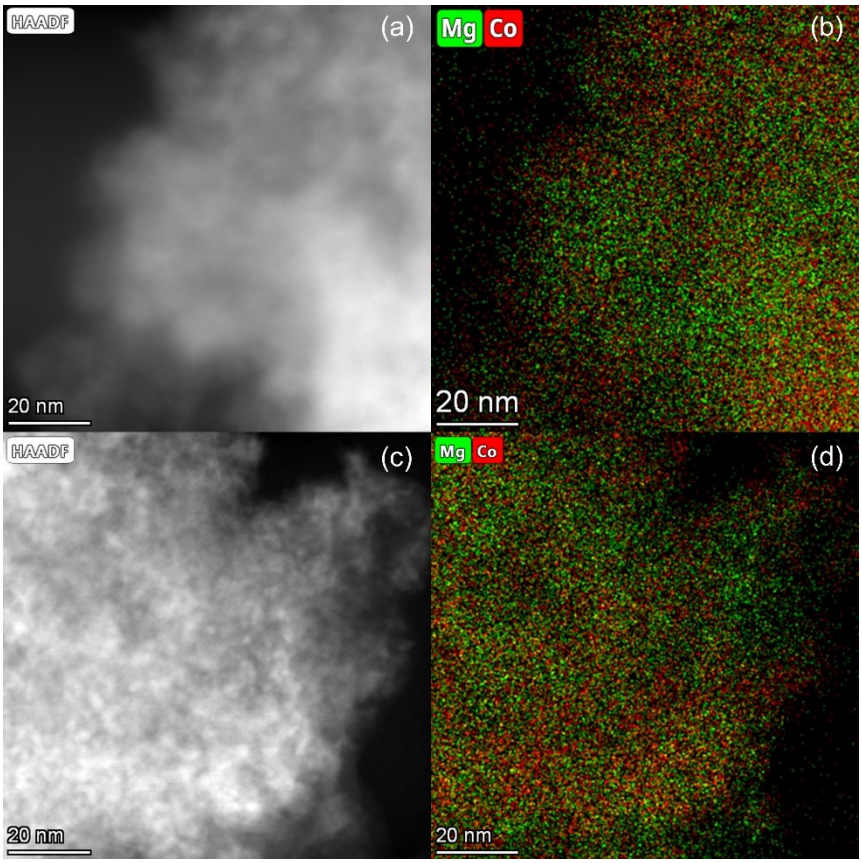

Figure S2. HAADF-STEM and STEM-EDX mapping images of the fresh (a and b) and spent catalysts (c and d).

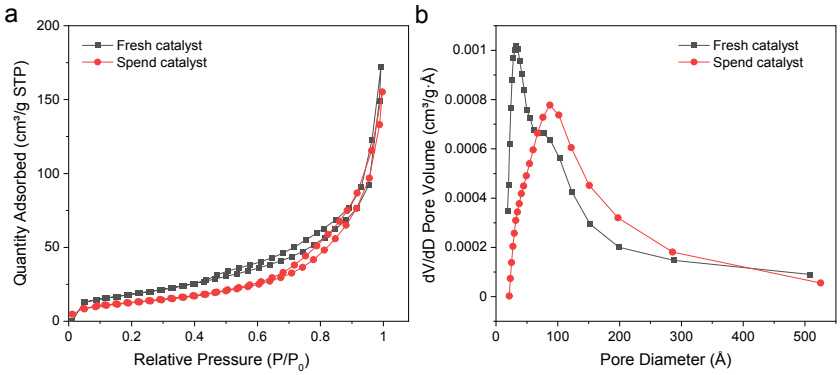

Figure S3. a) Nitrogen adsorption–desorption isotherms and b) BJH pore size distribution curves for fresh and spent LiH/Co-Mg-O-co catalysts.

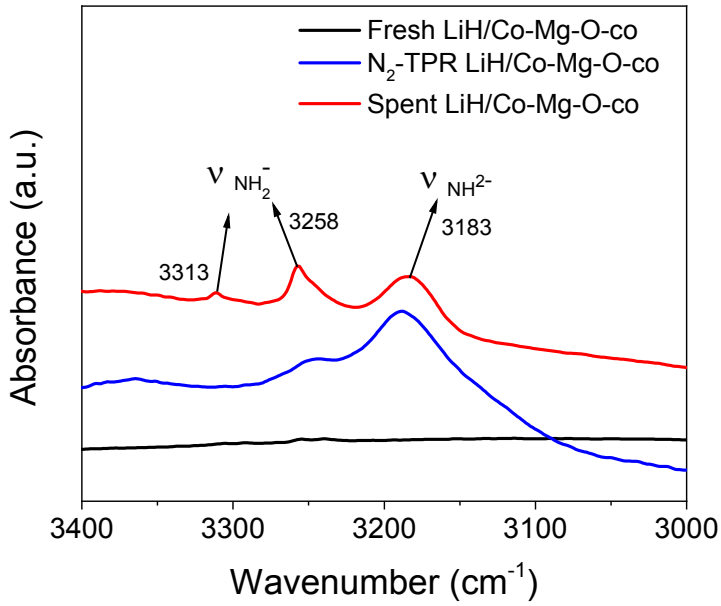

Figure S4. FTIR spectra of the fresh LiH/Co-Mg-O-co catalyst and the samples collected after activity test and N_2-TPR measurement. The IR bands at 3258 and 3313 cm^{-1} are the N–H stretching vibrations of $LiNH_2$ and the band at about 3183 cm^{-1} is the N–H stretching vibration of Li_2NH.[5-7]

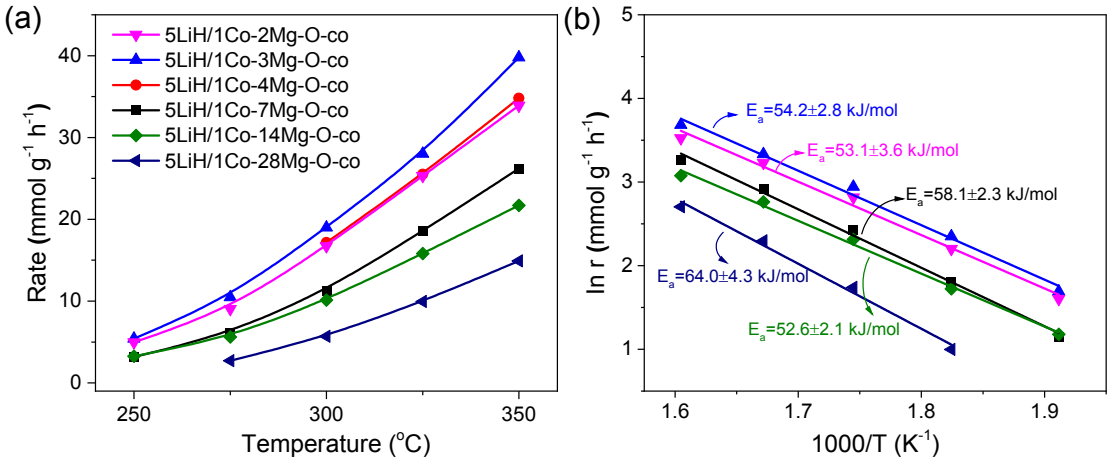

Figure S5. (a) Ammonia synthesis rates of a series of LiH/Co-*m*Mg-O-co catalysts. The molar ratio of LiH and Co was fixed at 5:1. Reaction conditions: syngas (N_2:H_2=1:3), WHSV=60000 mL g^{-1} h^{-1}, 10 bar. (b) Arrhenius plots of a series of LiH/Co-*m*Mg-O-co catalysts.

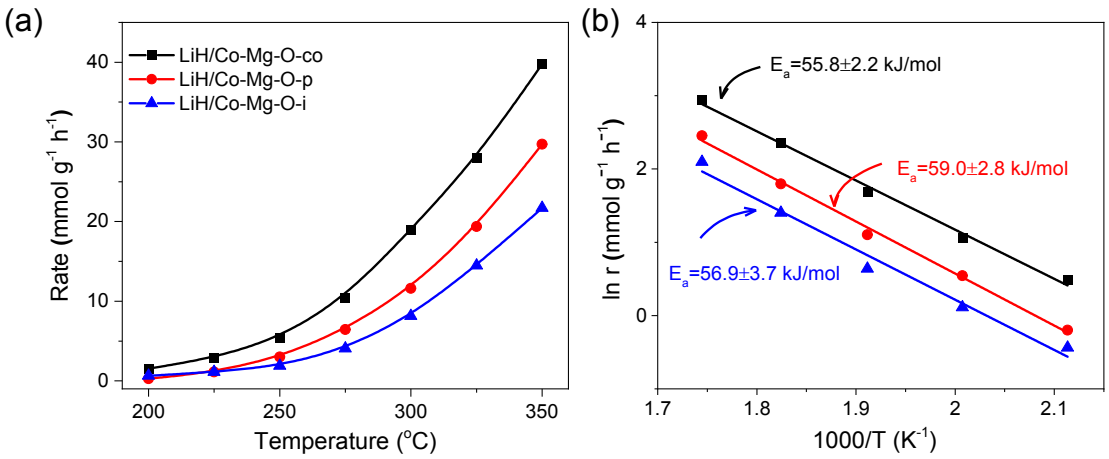

Figure S6. (a) Temperature dependence of ammonia synthesis rate over three different LiH/Co-Mg-O catalysts with different preparation methods, i.e., co-precipitation, precipitation, and impregnation (abbreviated as -co, -p, and -i, respectively) (b). Arrhenius plots of the three catalysts. The similar E_a values suggest the reaction mechanisms of ammonia synthesis over the three catalysts are the same.

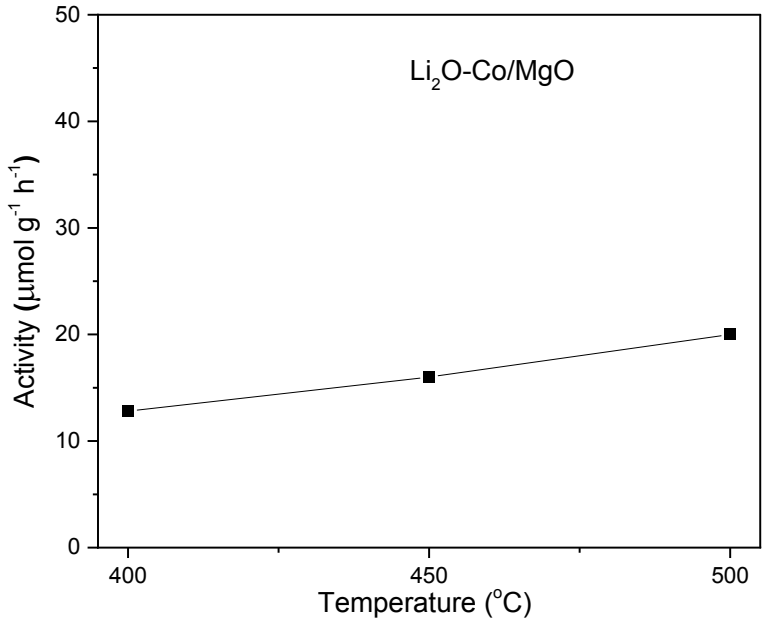

Figure S7. Temperature dependences of the catalytic performances over Li_2O-Co/MgO catalyst at 10 bar, 1:3 of N_2/H_2 and WHSV of 60000 mL g_{cat}^{-1} h^{-1}.

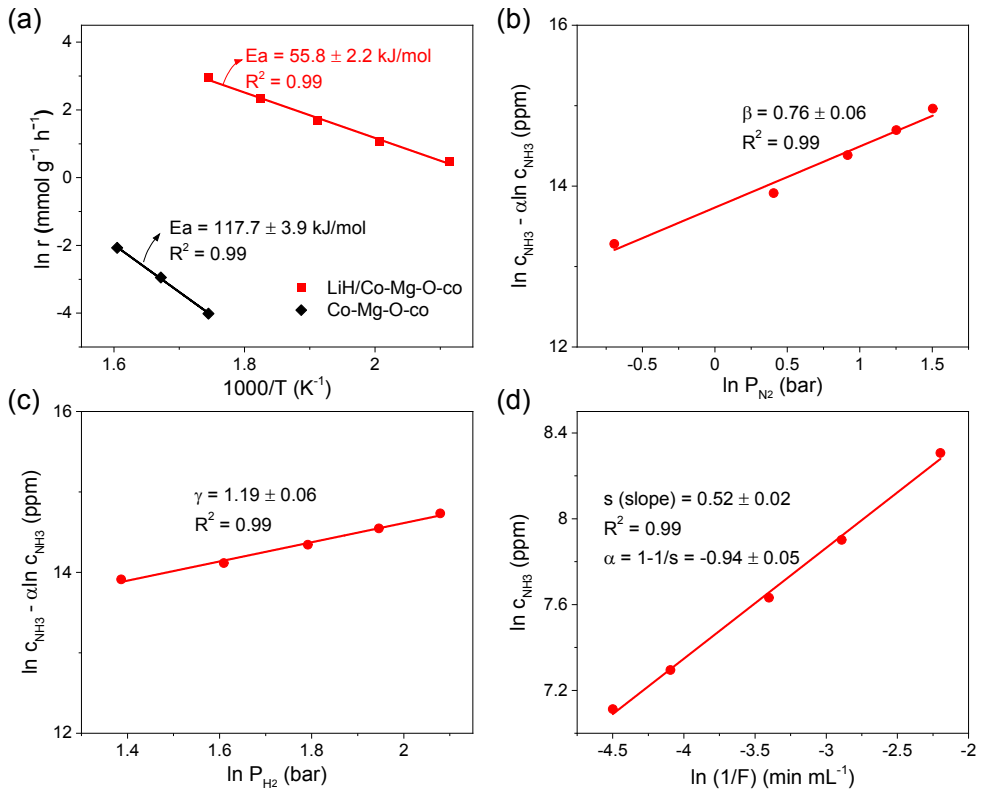

Figure S8. Kinetics studies of the LiH/Co-Mg-O-co. (a) Arrhenius plots and apparent activation energies (E_a) of the LiH/Co-Mg-O-co and Co-Mg-O-co catalysts, (b) N_2 reaction order of the LiH/Co-Mg-O-co catalyst, (c) H_2 reaction order of the LiH/Co-Mg-O-co catalyst, (d) NH_3 reaction order of the LiH/Co-Mg-O-co catalyst. The measurement of reaction orders was conducted at 250 °C and 10 bar. The effect of variation of P_{NH3} was considered.

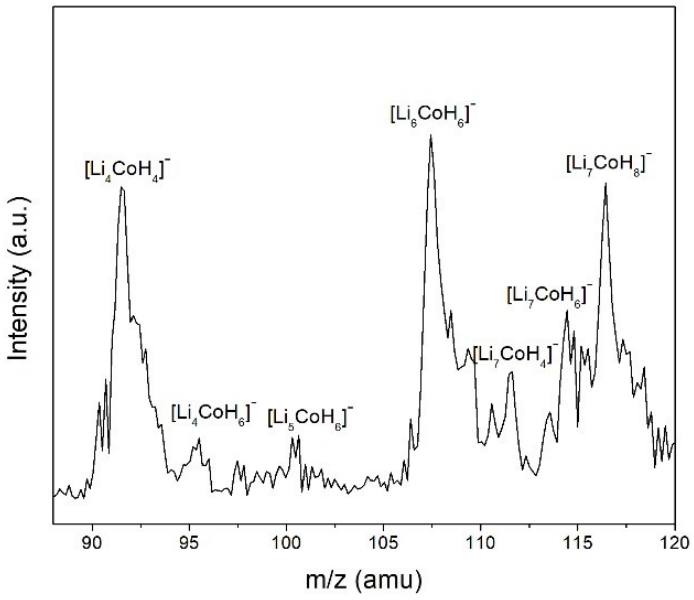

Figure S9. Mass spectrum of the [Li-Co-H] gas-phase cluster species produced by pulsed laser vaporization of the Co-LiH target in the presence of a He carrier gas.

Table S1. Properties of the Co-Based Catalysts.

Catalysts	Specific surface area	Co loading (wt %) [b]	Li loading (wt %) [b]	Co mean particle size (nm) [c]
LiH/Co-Mg-O-co	96.0	21.3	17.2	6.0
Co-LiH	42.5	59.6	35.4	27.6

[a]. Specific surface area was measured by N_2 physisorption at -196 °C and calculated according to the BET equation.

[b]. Co and Ba contents were determined by inductively coupled plasma atomic emission spectroscopy (ICP-AES).

[c]. Co mean particle size was calculated according to Scherer's formula.

Table S2. Ammonia synthesis over a series of Co- and Ru-based catalysts.

Catalysts	r_{NH_3} (mmol g^{-1} h^{-1})	NH_3 yield (%)	Reaction conditions	WHSV (mL g^{-1} h^{-1})	Ref.
LiH/Co-Mg-O	**19.0**	**1.55**	**300 °C, 10 bar**	**60000**	**This work**
	40.0	**3.25**	**350 °C, 10 bar**	**60000**	
LiH/Co-co	2.3	0.19	300 °C, 10 bar	60000	This work
Co-LiH	4.7	0.38	300 °C, 10 bar	60000	[2]
BaH_2-Co/CNTs	4.8	0.39	300 °C, 10 bar	60000	[8]
$Ba_{0.35}$-Co/C	9.0	0.73	320 °C, 10 bar	60000	[3]
Co/C12A7:e^-	3.8	1.04	400 °C, 9 bar	18000	[9]
LaCoSi	5.0	0.68	400 °C, 9 bar	36000	[10]
Cs/Co_3Mo_3N	5.0	2.72	400 °C, 11 bar	9000	[11]
Co/$BaTiO_{2.37}H_{0.63}$	3.0	0.22	400 °C, 10 bar	66000	[12]
Co/Ba-$Ca(NH_2)_2$	6.6	0.90	300 °C, 9 bar	36000	[13]
Cs-Ru/MgO	1.4	0.11	300 °C, 10 bar	60000	[2]
Ru/C12A7:e^-	0.76	0.10	300 °C, 9 bar	36000	[13]
Ru/Ca_2N:e^-	4.0	0.54	320 °C, 10 bar	36000	[14]
Ru/Pr_2O_3	1.0	0.27	310 °C, 9 bar	18000	[15]
Ru/$BaTiO_{2.5}H_{0.5}$	7.6	0.56	400 °C, 10 bar	66000	[12]
Ru/Ba-$Ca(NH_2)_2$	23.3	3.16	300 °C, 9 bar	36000	[13]

Table S3. Kinetic parameters of selected catalysts.

Catalysts	N_2 order (β)*	H_2 order (γ)*	NH_3 order (α)	E_a (kJ mol^{-1})	Ref.
LiH/Co-Mg-O	**0.40 (0.76)**	**0.62 (1.19)**	**-0.94**	**55.8 (200-300 °C)**	**This work**
Co-LiH	0.48 (1.0)	0.65 (1.4)	-1.2	52.1 (225-325 °C)	2
BaH_2-Co/CNTs	0.43 (0.64)	0.58 (0.81)	-0.41	58.0 (250-350 °C)	8
Co/C	0.8	-0.4	-0.3	149 (320-400 °C)	3
$Ba_{0.35}$-Co/C	0.9	1.5	-1.1	103 (320-400 °C)	3
Co_3Mo_3N	0.99	0.8	-1.34	56.5 (320-400 °C)	11
Co/C12A7:e^-	1.08 (1.08)	1.4 (1.4)	-1.18	49.5 (200-340 °C)	9
Cs-Ru/MgO	0.8 (0.8)	-0.9 (-0.9)	0	109 (277-257 °C)	16
Ru/C12A7:e^-	0.46 (0.9)	0.97 (1.9)	-1.0	90 (250-320 °C)	17
KM1	0.9	2.2	-1.5	70 (320-400 °C)	3

*The effect of the variation of P_{NH3} was considered for the reaction orders of N_2 and H_2 in the brackets.

References

1. H. Miyaoka, H. Fujii, H. Yamamoto, S. Hino, H. Nakanishi, T. Ichikawa and Y. Kojima, *Int J Hydrogen Energ*, 2012, **37**, 16025-16030.
2. P. Wang, F. Chang, W. Gao, J. Guo, G. Wu, T. He and P. Chen, *Nat. Chem.*, 2017, **9**, 64-70.
3. S. Hagen, R. Barfod, R. Fehrmann, C. J. H. Jacobsen, H. T. Teunissen and I. Chorkendorff, *J Catal*, 2003, **214**, 327-335.
4. P. K. Wang, H. Xie, J. P. Guo, Z. Zhao, X. T. Kong, W. B. Gao, F. Chang, T. He, G. T. Wu, M. S. Chen, L. Jiang and P. Chen, *Angew. Chem. Int. Ed.*, 2017, **56**, 8716-8720.
5. P. Chen, Z. Xiong, J. Luo, J. Lin and K. L. Tan, *J. Phys. Chem. B*, 2003, **107**, 10967.
6. J. Bohger, R. Essmann and H. Jacobs, *J. Mol. Struct.*, 1995, **348**, 325-328.
7. Y. Kojima and Y. Kawai, *J. Alloy. Compd.*, 2005, **395**, 236-239.
8. W. B. Gao, P. K. Wang, J. P. Guo, F. Chang, T. He, Q. R. Wang, G. T. Wu and P. Chen, *ACS Catal.*, 2017, **7**, 3654-3661.
9. Y. Inoue, M. Kitano, M. Tokunari, T. Taniguchi, K. Ooya, H. Abe, Y. Niwa, M. Sasase, M. Hara and H. Hosono, *ACS Catal.*, 2019, **9**, 1670-1679.
10. Y. T. Gong, J. Z. Wu, M. Kitano, J. J. Wang, T. N. Ye, J. Li, Y. Kobayashi, K. Kishida, H. Abe, Y. Niwa, H. S. Yang, T. Tada and H. Hosono, *Nat. Catal.*, 2018, **1**, 178-185.
11. R. Kojima and K. Aika, *Appl. Catal. A-Gen.*, 2001, **218**, 121.
12. Y. Tang, Y. Kobayashi, N. Masuda, Y. Uchida, H. Okamoto, T. Kageyama, S. Hosokawa, F. Loyer, K. Mitsuhara, K. Yamanaka, Y. Tamenori, C. Tassel, T. Yamamoto, T. Tanaka and H. Kageyama, *Adv Energy Mater*, 2018, **8**, 1801772.
13. M. Kitano, Y. Inoue, M. Sasase, K. Kishida, Y. Kobayashi, K. Nishiyama, T. Tada, S. Kawamura, T. Yokoyama, M. Hara and H. Hosono, *Angew. Chem. Int. Ed.* , 2018, **57**, 2648-2652.
14. M. Kitano, Y. Inoue, H. Ishikawa, K. Yamagata, T. Nakao, T. Tada, S. Matsuishi, T. Yokoyama, M. Hara and H. Hosono, *Chem. Sci.*, 2016, **7**, 4036-4043.
15. K. Sato, K. Imamura, Y. Kawano, S. Miyahara, T. Yamamoto, S. Matsumura and K. Nagaoka, *Chem. Sci.*, 2017, **8**, 674-679.
16. F. Rosowski, A. Hornung, O. Hinrichsen, D. Herein, M. Muhler and G. Ertl, *Appl. Catal. A-Gen.*, 1997, **151**, 443-460.
17. M. Kitano, S. Kanbara, Y. Inoue, N. Kuganathan, P. V. Sushko, T. Yokoyama, M. Hara and H. Hosono, *Nat. Commun.*, 2015, **6**, 6731.